# Difformer: Empowering Diffusion Model on Embedding Space for Text Generation

Zhujin Gao<sup>1\*</sup>, Junliang Guo<sup>2\*</sup>, Xu Tan<sup>2</sup>, Yongxin Zhu<sup>1</sup>, Fang Zhang<sup>1</sup>, Jiang Bian<sup>2</sup> and Linli Xu<sup>1</sup>

<sup>1</sup>University of Science and Technology of China, State Key Laboratory of Cognitive Intelligence <sup>2</sup>Microsoft Research Asia

<sup>1</sup>{gaozhujin, zyx2016, fangzhang}@mail.ustc.edu.cn, linlixu@ustc.edu.cn <sup>2</sup>{junliangguo, xuta, jiabia}@microsoft.com

### **Abstract**

Diffusion models have achieved state-of-theart synthesis quality on visual and audio tasks, and recent works adapt them to textual data by diffusing on the embedding space. But the difference between the continuous data space and the embedding space raises challenges to the diffusion model, which have not been carefully explored. In this paper, we conduct systematic studies and analyze the challenges threefold. Firstly, the data distribution is learnable for embeddings, which may lead to the collapse of the loss function. Secondly, as the norm of embedding varies between popular and rare words, adding the same noise scale will lead to sub-optimal results. In addition, we find that noises sampled from a standard Gaussian distribution may distract the diffusion process. To solve the above challenges, we propose Difformer, a denoising diffusion probabilistic model based on Transformer, which consists of three techniques including utilizing an anchor loss function, a layer normalization module for embeddings, and a norm factor to the Gaussian noise. All techniques are complementary to each other and critical to boosting the model performance together. Experiments are conducted on benchmark datasets over two seminal text generation tasks including machine translation and text summarization. The results show that Difformer significantly outperforms the embedding diffusion baselines, while achieving competitive results with strong autoregressive baselines.

#### 1 Introduction

A wave of diffusion models (Sohl-Dickstein et al., 2015; Ho et al., 2020) is sweeping the generation tasks (e.g., image and audio synthesis) recently, showing their great potential for high-quality data generation. Diffusion models are a family of iterative generative models, which are trained to recover corrupted data and then generate data by gradually

refining samples from the pure noise. This procedure enables the model to make subtle refinements of output samples in a multi-step denoising process, and thus generate high-fidelity samples (Rombach et al., 2022; Chen et al., 2020).

Besides booming achievements on vision (Song et al., 2020; Dhariwal and Nichol, 2021; Nichol and Dhariwal, 2021; Ho and Salimans, 2021; Rombach et al., 2022) and audio (Chen et al., 2020; Kong et al., 2020) generation, the exploration of diffusion model on text generation is still at an initial stage. Recent works (Li et al., 2022; Gong et al., 2022; Strudel et al., 2022) convert the discrete token to embeddings and then utilize continuous diffusion models to generate them, which can be termed embedding diffusion models. These initial attempts follow the original model to deal with the embeddings, with little consideration of the unique properties of the embedding data space which is learned from scratch.

In this paper, we provide a thorough study of the challenges of embedding diffusion models, which are divided into three-fold. Firstly, for diffusion models on image and audio generation, the ground truth data, i.e., the initial state of the forward diffusion process, is fixed during training. But it is learnable for textual data (i.e. embeddings), which may cause the collapse of the denoising loss function and bring instability to the training of the model. We analyze this problem in Section 3.1. Secondly, the long-tailed problem occurs widely in natural language processing (Schakel and Wilson, 2015), i.e., the imbalanced frequency of popular and rare words makes the learning of their embeddings diverge, which is illustrated in Section 3.2. As a result, the embedding scale of different words is diverse, and it would be sub-optimal to add the same scale of noise to embeddings in different scales. Thirdly, when denoising an embedding from a pure noise sampled from the normal Gaussian prior, it may fall to embeddings that are near the noise and

<sup>\*</sup>Equal contribution.

therefore distract the diffusion process. We show this phenomenon in Section 3.3.

To solve the above challenges, in this paper, we propose Difformer, a denoising diffusion Transformer model. Specifically, to avoid the collapse of the denoising loss function with moving embedding parameters, we propose an anchor loss function to stabilize the training process. Then, we introduce a layer normalization module on the top of the embedding layer to regularize the embeddings of popular and rare words into a uniform scale, eliminating the variant scales on them. In addition, to reduce the distraction brought by the noise, we increase the scale of the added Gaussian noise by introducing a hyper-parameter named the noise factor. We conduct experiments on two seminal text generation tasks including machine translation and text summarization. On all five benchmark datasets, Difformer largely outperforms original diffusion-based and iteration-based nonautoregressive baselines.

Our contributions can be summarized as follows:

- We provide thorough studies on several key problems revealed by continuous diffusion models on discrete text generation tasks, including the collapse of the denoising objective, the imbalanced scale over words, and the distraction brought by noise.
- We propose Difformer, a continuous diffusion model that solves the problems with three key components, i.e., an anchor loss function, a layer normalization module over the embeddings, and a noise factor that controls the scale of added Gaussian noise.
- We evaluate the performance of Difformer on machine translation and text summarization tasks, which consistently achieves better results in both generation quality and inference speed compared with original diffusion-based models.

#### 2 Background

**Diffusion Models** Denoising diffusion probabilistic models (Sohl-Dickstein et al., 2015; Ho et al., 2020) utilize a forward process to perturb the data with Gaussian noise step by step, and a reverse process to restore the data symmetrically. Ho et al. (2020) develop the approach by specific parameterizations and achieve comparable sample

quality with state-of-the-art generative models such as GANs (Goodfellow Ian et al., 2014). After that, great improvements have been made by many following works (Song et al., 2020; Dhariwal and Nichol, 2021; Nichol and Dhariwal, 2021; Rombach et al., 2022) both in quality and efficiency.

Specifically, given the data sample  $z_0 \in \mathbb{R}^d$ , the denoising diffusion probabilistic model (Ho et al., 2020) gradually perturbs it into a pure Gaussian noise  $z_T \sim \mathcal{N}(\mathbf{0}, \mathbf{I})$  through a series of latent variables  $z_T, \cdots, z_1$  in the forward process, and each step is a Markov transition:

$$q(\boldsymbol{z}_t|\boldsymbol{z}_{t-1}) = \mathcal{N}(\boldsymbol{z}_t; \sqrt{1-\beta_t}\boldsymbol{z}_{t-1}, \beta_t \mathbf{I}), \quad (1)$$

where  $\beta_t$  controls the noise level added at timestep t, and sampling arbitrary  $z_t$  from  $z_0$  can be obtained in a closed form:

$$q(\boldsymbol{z}_t|\boldsymbol{z}_0) = \mathcal{N}(\boldsymbol{z}_t; \sqrt{1 - \bar{\beta}_t} \boldsymbol{z}_0, \bar{\beta}_t \mathbf{I}),$$
 (2)

where  $\bar{\beta}_t := 1 - \prod_{i=0}^t (1 - \beta_i)$ . In the reverse process, the model recovers the data  $z_0$  by denoising from  $z_T$  with each step parameterized as:

$$p_{\theta}(\boldsymbol{z}_{t-1}|\boldsymbol{z}_t) = \mathcal{N}(\boldsymbol{z}_{t-1}; \boldsymbol{\mu}_{\theta}(\boldsymbol{z}_t, t), \boldsymbol{\Sigma}_{\theta}(\boldsymbol{z}_t, t)),$$
(3)

where  $\mu_{\theta}(\cdot)$  and  $\Sigma_{\theta}(\cdot)$  are the model predicted mean and covariance of  $q(z_{t-1}|z_t)$ , and  $\theta$  denotes the parameters of model. Following the derivation in Ho et al. (2020), we set  $\Sigma_{\theta}(z_t,t) = \sigma_t^2 \mathbf{I}$ . The objective function of the diffusion model is the variational lower-bound (VLB) of  $\log p_{\theta}(z_0)$ , which can be written as:

$$\mathcal{L}_{ ext{vlb}} = \mathbb{E}_{oldsymbol{z}_0,t} \left[ rac{1}{2\sigma_t^2} \left\| ilde{oldsymbol{\mu}}_t(oldsymbol{z}_t,oldsymbol{z}_0) - oldsymbol{\mu}_{ heta}(oldsymbol{z}_t,t) 
ight\|^2 
ight],$$

where  $\tilde{\mu}_t$  denotes the mean of  $q(z_{t-1}|z_t,z_0)$ . We further parameterize  $\mu_{\theta}(z_t,t) = \tilde{\mu}_t(z_t,\hat{z}_0)$ , where  $\hat{z}_0$  is the model prediction of the golden data  $z_0$ , i.e.,  $\hat{z}_0 = f_{\theta}(z_t,t)$ , and  $f_{\theta}(\cdot)$  represents the neural network. Then we could simplify the objective function as:

$$\mathcal{L}_{\text{vlb}} = \mathbb{E}_{\boldsymbol{z}_0, t} \left[ \| \hat{\boldsymbol{z}}_0 - \boldsymbol{z}_0 \|^2 \right]. \tag{4}$$

**Diffusion Models on Text Generation** The breakthrough of diffusion models on continuous data encourages people to explore their capacity on discrete textual data. Recent works mainly follow two lines. Firstly, discrete diffusion models (Hoogeboom et al., 2021; Austin et al., 2021a;

Savinov et al., 2021; Reid et al., 2022) that build on categorical distributions are proposed, in which sentences are corrupted and refined in the token level. Recent works have also explored modeling on surrogate representations of discrete data such as analog bits (Chen et al., 2022) and simplex (Han et al., 2022). These kinds of corruptions are coarsegrained and not able to model the semantic correlation between tokens.

In contrast, recent works (Li et al., 2022; Strudel et al., 2022; Gong et al., 2022) propose additional embedding and rounding steps in the forward and reverse process respectively to convert tokens into embeddings, and then utilize continuous diffusion models to add Gaussian noise controlled by a smooth schedule function to embeddings, achieving a fine-grained sampling process. Specifically, given a sequence of tokens y, the embedding step can be denoted as  $z_0 = \mathcal{N}(e(y), \beta_0 \mathbf{I})$  where  $e(\cdot)$ denotes the embedding lookup function, and the rounding step as  $p_{\theta}(y|z_0)$ , i.e., a softmax distribution over the vocabulary, with an extra loss function  $\mathcal{L}_{\text{round}} = -\log p_{\theta}(y|z_0)$  which is added to Equ (4). Nevertheless, these works directly adapt continuous diffusion models to embeddings, without considering the differences between the learnable embedding space and fixed image or audio data, as well as the unique properties of embeddings learned from the discrete textual corpus. And there is still a lack of comprehensive analysis of the challenges of embedding diffusion models especially on benchmark text generation tasks such as machine translation and text summarization.

## 3 Challenges of Diffusion Model on Embeddings

We analyze the challenges of utilizing continuous diffusion models on the embedding space in this section. We first introduce the experimental settings. We train diffusion models on the IWSLT14 German to English machine translation task, which is a commonly utilized benchmark dataset. The model architecture is based on Transformer (Vaswani et al., 2017). Given a source sentence  $x=[x_1,x_2,\cdots,x_m]$ , the encoder provides its hidden representation, which is taken as the condition of the decoder to generate the target sentence  $y=[y_1,y_2,\cdots,y_n]$ . The loss function is equivalent to Equ (4) with conditioning on x, i.e., model prediction as  $\hat{\boldsymbol{z}}_0=f_{\theta}(\boldsymbol{z}_t,t;x)$ .

Table 1: The anisotropy scores of embeddings learned by diffusion models with different loss functions.

$\mathcal{L}_{ ext{vlb}}$ w/ $\mathcal{L}_{ ext{round}}$	0.99
w/ $\mathcal{L}_{anchor}$	0.03

#### 3.1 Collapse of Denoising Objective

The data space is usually fixed for continuous data (e.g., image and audio), but is learned from scratch for discrete textual data (i.e., embeddings), which is therefore dynamic during training. Original diffusion models rely on the loss function in Equ (4) to learn the noise added to the data sample  $z_0$ . But the loss will collapse with jointly training both parts because the model can easily learn a trivial solution that all embeddings are similar to each other and all located in a small sub-region of the embedding space, which can be termed as anisotropic embeddings (Ethayarajh, 2019). Formally, we can measure the anisotropy of embeddings by computing the self-similarity score:

$$ANI = \frac{1}{C} \sum_{i=1}^{|V|} \sum_{j=1, j \neq i}^{|V|} \cos(e(i), e(j)), \quad (5)$$

where |V| is the vocabulary size of embeddings, and  $C = |V| \times (|V| - 1)$  indicates the total number of embedding pairs. The lower anisotropy, the better embeddings are. Because with higher scores, the embeddings of different tokens are less discriminative and non-uniformly distributed in the space, and thus limit the representation power of the model. We list the scores of embeddings learned by diffusion models with different loss functions in Table 1, where we find that with only  $\mathcal{L}_{\text{vlb}}$ , the embeddings are collapsed.

Recent works of diffusion model on embeddings (Li et al., 2022; Gong et al., 2022) introduce the rounding loss  $\mathcal{L}_{round}$  to alleviate this problem, which we find is not sufficient to provide strong constraints. In experiments, we find that the rounding loss descends drastically and falls to near zero in the first several steps. In addition, the anisotropy score of learned embeddings is still very high as shown in Table 1. The reason is that although  $\mathcal{L}_{round} = -\log p_{\theta}(y|z_0)$  is based on cross-entropy that can push different embeddings apart, it is too simple for the model to tackle as the input  $z_0$  is obtained from the original embedding e(y) with adding a small amount of noise. We have also tried to increase the weight of  $\mathcal{L}_{round}$  or the scale of the

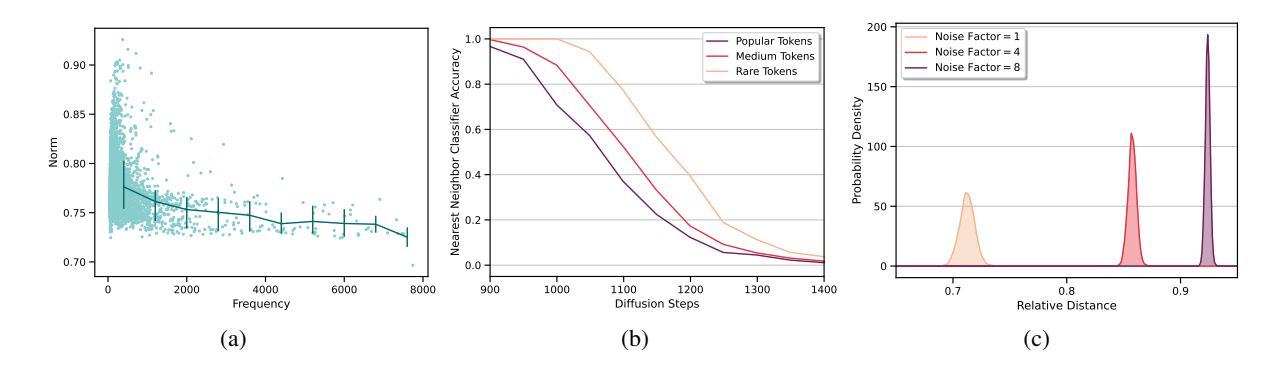


Figure 1: (a) Distribution of the embedding norm over token frequency. Embeddings of lower frequency tokens tend to have larger norms, while higher frequency ones have smaller norms. (b) The classification accuracy of whether the nearest neighbor of noisy embedding  $z_t$  is still  $z_0$  at different diffusion step t. Different lines indicate embeddings in different frequencies. (c) The distribution of the distance ratio from noise to embeddings. Noise Factor = 1 indicates the original diffusion model.

added noise, both of which do not solve the problem, however. Correspondingly, in experiments, we find that the model is not able to provide reasonable translation results with the rounding loss function.

#### 3.2 Imbalanced Embedding Scale

Due to the imbalanced frequency of tokens in natural language processing datasets, the token embeddings will have different exposures to the loss function as well as gradients, which will finally lead to different scales (i.e., L2 norms)<sup>1</sup> of learned embeddings. In Figure 1(a), we show the joint distribution of the token frequency and its embedding norm from a well-trained autoregressive baseline. We find that there exists a negative correlation between the norm and frequency of tokens, which indicates that embeddings of rare tokens are more likely to have large norms. Previous works also support our findings (Schakel and Wilson, 2015; Liu et al., 2020).

Based on this fact, it will be sub-optimal to add the same amount of noise to different embeddings, as embeddings with large norms require more noise to wipe out their intrinsic information, while it is the opposite for embeddings with small norms. As shown in Figure 1(b), when adding noises to embeddings of tokens in different frequencies, rare token embeddings need more steps to distinguish the noised results from them because of their larger scales, while popular token embeddings need less.

#### 3.3 Distraction in the Diffusion Process

In the reverse process of the diffusion model, noise is sampled from prior and generates the target embedding through a series of denoising steps. In this process, the generation results may be distracted by other embeddings that are near the noise. For example, the noise may fall to generate its nearest embedding if the distance is smaller than that between the noise and its target embedding.

We quantitatively analyze the distraction brought by noises in Figure 1(c). Specifically, given a target embedding  $e(y_i)$ , we sample a noise  $z_T$  from the prior and denote the nearest embedding to  $z_T$  as  $e(y_i')$ . We then calculate the ratio between  $d(z_T, e(y_i'))$  and  $d(z_T, e(y_i))$ , where  $d(\cdot, \cdot)$  is the L2 distance. A smaller ratio indicates that the noise is closer to the nearest embedding to it than the target one, therefore distracting the denoising process of the noise. As illustrated in Figure 1(c), the original prior brings a relatively larger amount of distraction to the denoising process.

# 4 Difformer: Denoising Diffusion Model based on Transformer

After illustrating the challenges of continuous diffusion models on embeddings, in this section, we introduce Difformer which solves the challenges with three novel techniques.

#### 4.1 The Anchor Loss Function

A straightforward solution to the first challenge is to replace the randomly initialized embedding matrix with a pre-trained one (e.g. embeddings from pre-trained language models such as BERT (Devlin et al., 2019)) and fix it during training. However,

<sup>&</sup>lt;sup>1</sup>We use the term scale and norm interchangeably in the rest of the paper.

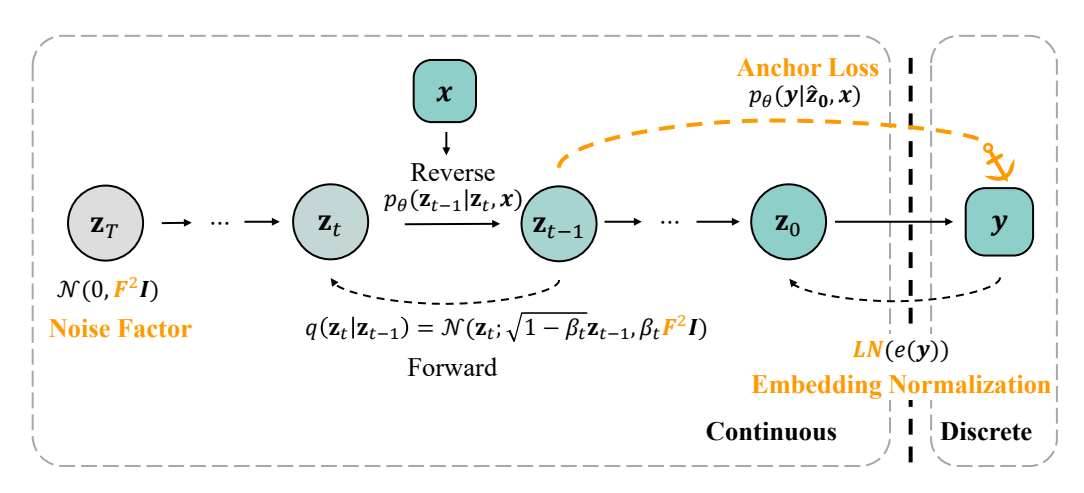


Figure 2: An overview of the proposed Difformer, illustrating the three main contributions, i.e., the anchor loss function, the embedding normalization, and the noise factor.

due to the difference between the loss functions and tasks, utilizing and fixing pre-trained embeddings is only a sub-optimal solution for diffusion models as verified in Table 3.

Instead, we propose a training objective term named anchor loss:

$$\mathcal{L}_{\text{anchor}} = -\log p_{\theta}(y|\hat{\boldsymbol{z}}_0). \tag{6}$$

Comparing with  $\mathcal{L}_{\mathrm{round}},$   $\mathcal{L}_{\mathrm{anchor}}$  utilizes the model prediction  $\hat{z}_0$  as input instead of the golden embedding  $z_0$ . Intuitively, while both aim at pushing embeddings apart to prevent the collapse of the denoising objective,  $\mathcal{L}_{\mathrm{round}}$  uses the noisy embedding  $z_0 = \mathcal{N}(e(y), \beta_0 \mathbf{I})$  to predict the embedding e(y), where the distance between  $z_0$  and e(y) is too small to provide useful guidance. While in  $\mathcal{L}_{\mathrm{anchor}}$ , by using the model output  $\hat{\boldsymbol{z}}_0$  which is far from golden embeddings in the initial training stage, the loss successfully helps regularize embeddings and prevent  $\mathcal{L}_{\text{vlb}}$  from collapse. As a result, the anisotropic score of the embeddings learned by  $\mathcal{L}_{anchor}$  is very low as shown in Table 1, indicating that the embeddings are informative and discriminative to each other.

#### 4.2 Layer Normalization on Embeddings

To deal with the imbalanced embedding scales, we introduce a layer normalization module on the top of the embedding layer to ensure the uniform scale of tokens. Specifically, for embedding  $e(y_i)$  of token  $y_i$ , the module re-scales its distribution by:

$$LN(e(y_i)) = \frac{e(y_i) - \mathbb{E}[e(y_i)]}{\sqrt{\mathbb{V}[e(y_i] + \epsilon}} \odot \gamma + \eta,$$

where  $\odot$  denotes element-wise multiplication,  $\mathbb{E}[\cdot]$  and  $\mathbb{V}[\cdot]$  indicate expectation and variance respec-

tively,  $\gamma$  and  $\eta$  are learnable parameters that have the same size as the embedding dimension, and  $\epsilon$  is a small number to prevent overflow.

In consequence, as the parameters  $\gamma$  and  $\eta$  are shared across all embeddings, embeddings of different tokens will be normalized into the same scale, which eliminates the imbalanced scale problem illustrated in Section 3.2.

#### 4.3 The Noise Factor

To alleviate the distraction brought by other nontarget embeddings in the reverse process, we propose a simple but effective method by manually magnifying the scale of noise added at each step. Concretely, we generalize the covariance matrix of  $q(z_t|z_{t-1})$  from  $\beta_t \mathbf{I}$  to  $\beta_t F^2 \mathbf{I}$ , where F is a hyperparameter termed as noise factor. Formally, each forward step in Equ (1) can be written as:

$$q(\boldsymbol{z}_t|\boldsymbol{z}_{t-1}) = \mathcal{N}(\boldsymbol{z}_t; \sqrt{1-\beta_t}\boldsymbol{z}_{t-1}, \beta_t F^2 \mathbf{I}).$$
 (7)

Correspondingly, the prior becomes to  $p(z_T) = \mathcal{N}(\mathbf{0}, F^2\mathbf{I})$ , where F = 1 is equivalent to the original prior.

In this way, the distances of the sampled noises and embeddings are largely increased, then the difference from noises to embeddings will be reduced, i.e., different embeddings are similar from the view of noises with large noise factors. As shown in Figure 1(c), the ratio is increased with large noise factors, showing that the distances from the noise to the target and the nearest embeddings are similar, therefore reducing the distraction brought by it.

#### 4.4 Training and Inference

**Training objective** Given a source sentence  $x = [x_1, x_2, \dots, x_m]$ , the model learns to generate the

target sentence  $y=[y_1,y_2,\cdots,y_n]$  by estimating  $p_{\theta}(y|x)$ . Traditional models (Vaswani et al., 2017) factorize the distribution in an autoregressive way and estimate tokens with left-to-right sequential conditions, i.e.,  $p_{\theta}(y|x) = \prod_{i=1}^n p_{\theta}(y_i|y_{< i},x)$ . Diffusion models (Gong et al., 2022; Strudel et al., 2022) break the conditional dependency between tokens and estimate all tokens simultaneously in a non-autoregressive way (Gu et al., 2018), i.e.,  $p_{\theta}(y|x) = \prod_{i=1}^n p_{\theta}(y_i|z,x)$ . Then the final objective function of our model can be written as:

$$\mathcal{L} = \mathbb{E}_{(x,y),\boldsymbol{z}_0,t} \left[ \|\hat{\boldsymbol{z}}_0 - \boldsymbol{z}_0\|^2 - \log p_{\theta}(y|\hat{\boldsymbol{z}}_0) \right], \tag{8}$$

where the first and second items refer to  $\mathcal{L}_{vlb}$  and  $\mathcal{L}_{anchor}$  respectively.

#### Length Prediction and 2D Parallel Decoding

Unlike traditional autoregressive models where the sequence length is implicitly modeled by the generation of the EOS token, diffusion models generate all tokens in a non-autoregressive manner, where the length should be modeled explicitly. Previous works (Li et al., 2022; Gong et al., 2022; Strudel et al., 2022) usually generate a sequence with maximum length and cutoff the content after the EOS token. In this paper, we utilize a more efficient way by explicitly predicting the target length with the encoder output (Lee et al., 2018), i.e.,  $p_{\theta}(n|x)$ , and the negative log-likelihood loss function is added to Equ (8) while training.

A unique benefit of this approach is that we can conduct 2D parallel decoding in inference. Firstly, we can consider top- $b_1$  lengths from the length predictor to generate candidates with different lengths. Secondly, for each length, we can also generate  $b_2$  candidates by sampling different initial noises from the prior. The final prediction is selected from the total  $b = b_1 \times b_2$  candidates that minimize the expected risk (Kumar and Byrne, 2004) w.r.t a metric such as BLEU or PPL. We term  $b_1$  and  $b_2$  as length and noise beams respectively.

**Acceleration in Inference** Diffusion models are trained with thousands of forward steps, but it would be extremely time-consuming to utilize all steps in inference. For Difformer, we pick a subset  $\{\tau_1, \tau_2, \cdots, \tau_K\}$  of the full diffusion trajectory  $\{1, 2, \cdots, T\}$  for generation (Song et al., 2020; Nichol and Dhariwal, 2021). Then a reverse step

can be obtained by:

$$\boldsymbol{z}_{\tau_{i-1}} \sim q(\boldsymbol{z}_{\tau_{i-1}}|\boldsymbol{z}_{\tau_i}, \hat{\boldsymbol{z}}_0),$$
 (9)

$$\hat{\boldsymbol{z}}_0 = \hat{\boldsymbol{z}}_0(\boldsymbol{z}_{\tau_i}, \tau_i). \tag{10}$$

#### 5 Experiments

To evaluate the proposed Difformer model, we conduct experiments on two conditional text generation tasks including neural machine translation and text summarization.

#### 5.1 Experimental Setup

**Datasets** For machine translation, we consider three benchmark datasets including IWSLT14 German-English (IWSLT De-En), English-German (WMT En-De), and WMT16 English-Romanian (WMT En-Ro), mainly follow previous works (Gu et al., 2018; Guo et al., 2019; Ghazvininejad et al., 2019). For text summarization, we conduct experiments on Gigaword (Rush et al., 2017) and CNN/DM (Nallapati et al., 2016), two benchmark abstractive summarization datasets. Following previous non-autoregressive text generation works (Gu et al., 2018, 2019; Ghazvininejad et al., 2019), we adopt sequence-level knowledge distillation (Kim and Rush, 2016) to distill the original training set to alleviate the multi-modality problem. We use the distilled training set for WMT datasets and the original ones for other datasets.

**Baselines** We mainly compare our method with Diff-LM (Li et al., 2022), the embedding diffusion baseline that is originally designed for controllable text generation. We initialize its embeddings with BERT and fix it during training, cause we find that the model will crash if training embeddings from scratch or tuning it. We also include CMLM (Ghazvininejad et al., 2019), a conditional masked language model with iterative decoding, which can also be considered as a discrete diffusion model (Austin et al., 2021b). We initialize its embeddings with the pre-trained BERT model to ensure fair comparisons. We also include a concurrent work CDCD (Dieleman et al., 2022) as the baseline. In addition, we report the performance of the autoregressive Transformer baseline model.

**Implementation Details** We build our model on Transformer (Vaswani et al., 2017), and use transformer-iwslt-de-en config ( $n_{\rm layers}=6, n_{\rm heads}=4, d_{\rm hidden}=512, d_{\rm FFN}=1024$ ) for the IWSLT dataset, while transformer-base

Table 2: The performance of the proposed Difformer and the baseline methods, including BLEU scores on WMT14 En-De, WMT16 En-Ro, and IWSLT14 De-En, as well as ROUGE-1/2/L scores on Gigaword and CNN/DM. " $\uparrow$ " indicates the improvement of the Difformer over baselines with the same beam size b is significant at the level of 0.01. The baseline scores are all reported by our own implementations except CDCD.

Models	WMT14 En-De	WMT16 En-Ro	IWSLT14 De-En	Gigaword
Transformer ( $b = 1$ ) (Vaswani et al., 2017)	26.37	33.93	32.62	36.78/17.79/34.10
Transformer ( $b = 5$ )	27.37	34.72	33.91	37.54/18.80/34.93
CMLM $(b=1)$ (Ghazvininejad et al., 2019) CMLM $(b=10)$ Diff-LM $(b=1)$ (Li et al., 2022) Diff-LM $(b=10)$ CDCD $(b=1)$ (Dieleman et al., 2022) CDCD $(b=10)$	25.92 26.75 15.81 17.72 19.30 19.70	32.59 33.70 20.48 23.45 /	26.41 31.76 24.67 26.70	34.41/15.61/32.17 36.33/17.82/33.83 31.39/12.01/28.66 33.26/13.99/30.56
Difformer $(b = 1)$	26.47 <sup>↑</sup> 26.98 <sup>↑</sup> <b>27.10</b>	32.78 <sup>↑</sup>	31.16 <sup>↑</sup>	35.45/16.46/32.87 <sup>↑</sup>
Difformer $(b = 10)$		34.20 <sup>↑</sup>	33.52 <sup>↑</sup>	37.04/18.07/34.54 <sup>↑</sup>
Difformer $(b = 20)$		<b>34.23</b>	<b>33.74</b>	37.34/18.36/34.63

 $(n_{\mathrm{layers}}=6, n_{\mathrm{heads}}=8, d_{\mathrm{hidden}}=512, d_{\mathrm{FFN}}=2048)$  for other datasets. We set diffusion step T=2000, noise factor F=4, and use a linear noise schedule. Following previous works (Li et al., 2022; Strudel et al., 2022), we also utilize the self-conditioning (Chen et al., 2022) trick which is shown effective to improve the final performance. The training cost nearly one day on 8 Nvidia V100 GPUs. We downsample the diffusion step to 20 in inference, i.e., K=20, which is ten times faster than previous works (Li et al., 2022; Gong et al., 2022).

We initialize the embeddings by that in the pretrain bert-base-multilingual model for machine translation tasks, and bert-base for summarization tasks. To achieve that, we tokenize sentences and segment each token into subwords by WordPiece (Devlin et al., 2019), and we eliminate tokens that do not appear in our training sets. In evaluation, we report the tokenized BLEU score (Papineni et al., 2002) for machine translation results, and ROUGE score (Lin, 2004) for summarization.

#### 5.2 Results

The main results are listed in Table 2. With a little abuse of notation, we use b to represent the size of beam search for the Transformer baseline, as well as the size of parallel decoding (i.e.,  $b=b_1\times b_2$ ) of other models. From the results, the proposed Difformer outperforms both diffusion-based and iteration-based baselines on all datasets as well as different choices of b, and perform comparably with the autoregressive Transformer model. Specif-

Table 3: The ablation study on the proposed different components. Results are conducted on the IWSLT De-En task. "/" indicates the setting does not converge.

Models	BLEU
(1): Difformer (2): (1) w/o $\mathcal{L}_{anchor}$	33.74
(3): (1) w/o $\mathcal{L}_{anchor}$ w/ Fix Emb (4): (1) w/o Embedding Normalization	29.38 33.32
(5): (1) w/o Noise Factor	32.77

ically, Difformer brings significant improvements over the original Diff-LM model, indicating the challenges that continuous diffusion models meet on text generation tasks and the effectiveness of the proposed solutions. Compared with CMLM, an iteration-based non-autoregressive baseline, Difformer outperforms on different datasets consistently. Moreover, benefiting from the stochastic nature of diffusion models, Difformer is able to conduct 2D parallel decoding over the length and noise beam at the same time, increasing the diversity and potential to obtain better results. In contrast, the deterministic CMLM can only utilize different lengths, and we observe a performance drop when b is larger than 10.

#### **5.3** Ablation Study

We study whether the proposed different components benefit the model in this section. The results of the ablation study are listed in Table 3. Firstly, we find that the original Diff-LM (Li et al., 2022) model cannot be directly adapted to the considered text generation tasks, as we find that the model is collapsed under setting (2). This result echoes our

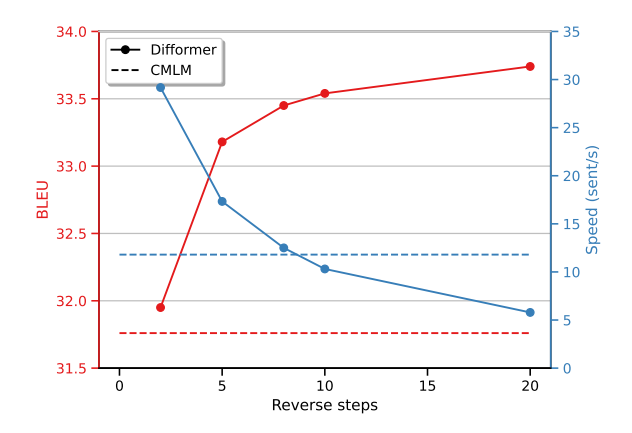


Figure 3: The results of varying the reverse step K. We set b=10 for Difformer and CMLM. The inference speed is measured by the number of generated sentences per second, and the higher the faster. Dashed lines indicate the results of the CMLM model.

Table 4: The analyse on  $b_1$  and  $b_2$ . Results are conducted on the IWSLT De-En task.

$b_1$	$b_2$	BLEU
9	5	33.74
9	1	33.52
4	5	32.79
4	1	32.68

findings in Section 3.1 that the rounding loss provides insufficient regularization to the embedding parameters.

We find two ways that can alleviate this problem, i.e., by either initializing the embeddings with BERT and then fixing them, or proposing an extra loss function  $\mathcal{L}_{anchor}$  that provides regularization to the model parameters. As a result, both methods are effective in solving the problem. But due to the differences between the model architecture and tasks, the pre-trained embedding only leads to sub-optimal solutions, while the proposed  $\mathcal{L}_{anchor}$  provides better results. Finally, the proposed noise factor and embedding normalization also help improve the model performance, bringing 0.93 and 0.42 gains on BLEU score respectively.

#### 5.4 Analyses

We provide fine-grained analyses of the hyperparameters in this section.

**Study on Reverse Steps** K Continuous diffusion models usually rely on a large number of reverse steps in inference to guarantee the quality of generated samples, so do recent works on text (either hundreds (Li et al., 2022) or thousands (Gong

et al., 2022; Strudel et al., 2022)). In contrast, we find that Difformer is able to achieve considerably good performance with only a few reverse steps. In Figure 3, we show the BLEU score and inference speed of Difformer by varying the reverse step Kfrom 2 to 20, with CMLM as a comparison. The conclusions are two-fold: 1) Difformer performs robust w.r.t K, and still outperforms CMLM even with only 2 reverse steps. We attribute this to the introduction of the anchor loss  $\mathcal{L}_{anchor}$ , which boost the prediction accuracy of  $\hat{z}_0$  especially when tis large. 2) Correspondingly, the inference speed of Difformer also outperforms the iterative nonautoregressive CMLM model by 3 times when Kis small, showing the potential of deploying Difformer to online systems.

**Study on**  $b_1$  **and**  $b_2$  We study the influence of the 2D parallel decoding hyper-parameters, i.e., the length beam size  $b_1$  and noise beam size  $b_2$  described in Section 4.4. As shown in Table 4, we find that length and noise beam are complementary to each other, and both of them boost the generation quality, while the length beam brings more significant improvements.

Experiments on Word Similarity We also evaluate the performance of learned embeddings on the RG65 dataset (Rubenstein and Goodenough, 1965) of the word similarity task, which evaluates whether the most similar word of a given word (using cosine similarity) is consistent with the ground truth, with Spearman correlation as the metric. We average the embeddings of subwords in our model to obtain the word embeddings. As a result, the Diff-LM baseline gets 31.89 while our model gets 39.11 points, showing that the proposed methods significantly improve the quality of embedding representations.

#### 6 Conclusion

In this paper, we first study the challenges of continuous embedding diffusion models, which are concluded in threefold: 1) the embedding space is learnable instead of fixed during training, which brings the collapse of denoising objective function; 2) the imbalanced embedding norms of popular and rare tokens make the uniform noise a sub-optimal choice; 3) the normal Gaussian noise introduces distraction to results. We propose Difformer, a denoising diffusion model based on Transformer to solve the challenges. Specifically, we introduce

an anchor loss function to regularize the model parameters, a layer normalization module on the top of embeddings, and a noise factor to increase the amount of noise added at each step, to deal with the challenges respectively. On two seminal text generation tasks including machine translation and text generation, Difformer outperforms previous diffusion-based models as well as an iterative non-autoregressive model. In the future, we plan to explore whether the proposed techniques also bring improvements in continuous data types such as image and audio.

#### References

- Jacob Austin, Daniel D Johnson, Jonathan Ho, Daniel Tarlow, and Rianne van den Berg. 2021a. Structured denoising diffusion models in discrete state-spaces. *Advances in Neural Information Processing Systems*, 34:17981–17993.
- Jacob Austin, Daniel D. Johnson, Jonathan Ho, Daniel Tarlow, and Rianne van den Berg. 2021b. Structured denoising diffusion models in discrete state-spaces. In Advances in Neural Information Processing Systems 34: Annual Conference on Neural Information Processing Systems 2021, NeurIPS 2021, December 6-14, 2021, virtual, pages 17981–17993.
- Nanxin Chen, Yu Zhang, Heiga Zen, Ron J Weiss, Mohammad Norouzi, and William Chan. 2020. Wavegrad: Estimating gradients for waveform generation. In *International Conference on Learning Representations*.
- Ting Chen, Ruixiang Zhang, and Geoffrey Hinton. 2022. Analog bits: Generating discrete data using diffusion models with self-conditioning. *arXiv* preprint arXiv:2208.04202.
- Jacob Devlin, Ming-Wei Chang, Kenton Lee, and Kristina Toutanova. 2019. BERT: Pre-training of deep bidirectional transformers for language understanding. In *Proceedings of the 2019 Conference of the North American Chapter of the Association for Computational Linguistics: Human Language Technologies, Volume 1 (Long and Short Papers)*, pages 4171–4186, Minneapolis, Minnesota. Association for Computational Linguistics.
- Prafulla Dhariwal and Alexander Nichol. 2021. Diffusion models beat gans on image synthesis. *Advances in Neural Information Processing Systems*, 34:8780–8794
- Sander Dieleman, Laurent Sartran, Arman Roshannai, Nikolay Savinov, Yaroslav Ganin, Pierre H. Richemond, Arnaud Doucet, Robin Strudel, Chris Dyer, Conor Durkan, Curtis Hawthorne, Rémi Leblond, Will Grathwohl, and Jonas Adler. 2022. Continuous diffusion for categorical data. *CoRR*, abs/2211.15089.

- Kawin Ethayarajh. 2019. How contextual are contextualized word representations? comparing the geometry of bert, elmo, and gpt-2 embeddings. *arXiv* preprint arXiv:1909.00512.
- Marjan Ghazvininejad, Omer Levy, Yinhan Liu, and Luke Zettlemoyer. 2019. Mask-predict: Parallel decoding of conditional masked language models. arXiv preprint arXiv:1904.09324.
- Shansan Gong, Mukai Li, Jiangtao Feng, Zhiyong Wu, and LingPeng Kong. 2022. Diffuseq: Sequence to sequence text generation with diffusion models. *arXiv preprint arXiv:2210.08933*.
- J Goodfellow Ian, Pouget-Abadie Jean, Mirza Mehdi, Xu Bing, Warde-Farley David, Ozair Sherjil, and C Courville Aaron. 2014. Generative adversarial nets. In *Proceedings of the 27th international conference on neural information processing systems*, volume 2, pages 2672–2680.
- Jiatao Gu, James Bradbury, Caiming Xiong, Victor OK Li, and Richard Socher. 2018. Non-autoregressive neural machine translation. In *International Conference on Learning Representations*.
- Jiatao Gu, Changhan Wang, and Junbo Zhao. 2019. Levenshtein transformer. *Advances in Neural Information Processing Systems*, 32.
- Junliang Guo, Xu Tan, Di He, Tao Qin, Linli Xu, and Tie-Yan Liu. 2019. Non-autoregressive neural machine translation with enhanced decoder input. In *Proceedings of the AAAI conference on artificial intelligence*, volume 33, pages 3723–3730.
- Xiaochuang Han, Sachin Kumar, and Yulia Tsvetkov. 2022. Ssd-lm: Semi-autoregressive simplex-based diffusion language model for text generation and modular control. *arXiv* preprint arXiv:2210.17432.
- Jonathan Ho, Ajay Jain, and Pieter Abbeel. 2020. Denoising diffusion probabilistic models. Advances in Neural Information Processing Systems, 33:6840–6851.
- Jonathan Ho and Tim Salimans. 2021. Classifier-free diffusion guidance. In NeurIPS 2021 Workshop on Deep Generative Models and Downstream Applications.
- Emiel Hoogeboom, Didrik Nielsen, Priyank Jaini, Patrick Forré, and Max Welling. 2021. Argmax flows and multinomial diffusion: Learning categorical distributions. *Advances in Neural Information Processing Systems*, 34:12454–12465.
- Yoon Kim and Alexander M Rush. 2016. Sequence-level knowledge distillation. *arXiv* preprint *arXiv*:1606.07947.
- Zhifeng Kong, Wei Ping, Jiaji Huang, Kexin Zhao, and Bryan Catanzaro. 2020. Diffwave: A versatile diffusion model for audio synthesis. In *International Conference on Learning Representations*.

- Shankar Kumar and William Byrne. 2004. Minimum bayes-risk decoding for statistical machine translation. Technical report, JOHNS HOPKINS UNIV BALTIMORE MD CENTER FOR LANGUAGE AND SPEECH PROCESSING (CLSP).
- Jason Lee, Elman Mansimov, and Kyunghyun Cho. 2018. Deterministic non-autoregressive neural sequence modeling by iterative refinement. In Proceedings of the 2018 Conference on Empirical Methods in Natural Language Processing, pages 1173–1182.
- Xiang Lisa Li, John Thickstun, Ishaan Gulrajani, Percy Liang, and Tatsunori B Hashimoto. 2022. Diffusion-lm improves controllable text generation. *arXiv* preprint arXiv:2205.14217.
- Chin-Yew Lin. 2004. Rouge: A package for automatic evaluation of summaries. In *Text summarization branches out*, pages 74–81.
- Xuebo Liu, Houtim Lai, Derek F Wong, and Lidia S Chao. 2020. Norm-based curriculum learning for neural machine translation. In *Proceedings of the 58th Annual Meeting of the Association for Computational Linguistics*, pages 427–436.
- Ramesh Nallapati, Bowen Zhou, Caglar Gulcehre, Bing Xiang, et al. 2016. Abstractive text summarization using sequence-to-sequence rnns and beyond. arXiv preprint arXiv:1602.06023.
- Alexander Quinn Nichol and Prafulla Dhariwal. 2021. Improved denoising diffusion probabilistic models. In *International Conference on Machine Learning*, pages 8162–8171. PMLR.
- Kishore Papineni, Salim Roukos, Todd Ward, and Wei-Jing Zhu. 2002. Bleu: a method for automatic evaluation of machine translation. In *Proceedings of the* 40th annual meeting of the Association for Computational Linguistics, pages 311–318.
- Machel Reid, Vincent J Hellendoorn, and Graham Neubig. 2022. Diffuser: Discrete diffusion via edit-based reconstruction. *arXiv preprint arXiv:2210.16886*.
- Robin Rombach, Andreas Blattmann, Dominik Lorenz, Patrick Esser, and Björn Ommer. 2022. High-resolution image synthesis with latent diffusion models. In *Proceedings of the IEEE/CVF Conference on Computer Vision and Pattern Recognition*, pages 10684–10695.
- Herbert Rubenstein and John B Goodenough. 1965. Contextual correlates of synonymy. *Communications of the ACM*, 8(10):627–633.
- Alexander M Rush, SEAS Harvard, Sumit Chopra, and Jason Weston. 2017. A neural attention model for sentence summarization. In ACLWeb. Proceedings of the 2015 conference on empirical methods in natural language processing.

- Nikolay Savinov, Junyoung Chung, Mikolaj Binkowski, Erich Elsen, and Aaron van den Oord. 2021. Step-unrolled denoising autoencoders for text generation. In *International Conference on Learning Representations*.
- Adriaan MJ Schakel and Benjamin J Wilson. 2015. Measuring word significance using distributed representations of words. arXiv preprint arXiv:1508.02297.
- Jascha Sohl-Dickstein, Eric Weiss, Niru Maheswaranathan, and Surya Ganguli. 2015. Deep unsupervised learning using nonequilibrium thermodynamics. In *International Conference on Machine Learning*, pages 2256–2265. PMLR.
- Jiaming Song, Chenlin Meng, and Stefano Ermon. 2020. Denoising diffusion implicit models. In *International Conference on Learning Representations*.
- Robin Strudel, Corentin Tallec, Florent Altché, Yilun Du, Yaroslav Ganin, Arthur Mensch, Will Grathwohl, Nikolay Savinov, Sander Dieleman, Laurent Sifre, et al. 2022. Self-conditioned embedding diffusion for text generation. *arXiv preprint arXiv:2211.04236*.
- Ashish Vaswani, Noam Shazeer, Niki Parmar, Jakob Uszkoreit, Llion Jones, Aidan N Gomez, Łukasz Kaiser, and Illia Polosukhin. 2017. Attention is all you need. *Advances in neural information processing systems*, 30.